

# Soft-Molecular Imprinted Electrospun Scaffolds to mimic specific biological tissues

Giuseppe Criscenti<sup>1,2,#</sup>, Carmelo De Maria<sup>1,#</sup>, Alessia Longoni<sup>2</sup>, Clemens A. van Blitterswijk<sup>2,3</sup>, Hugo A.M. Fernandes<sup>4</sup>, Giovanni Vozzi<sup>1</sup>, and Lorenzo Moroni<sup>2,3\*</sup>

<sup>1</sup> Research Center E. Piaggio and Department of Ingegneria dell'Informazione, University of Pisa, Pisa, Italy

<sup>2</sup> Department of Tissue Regeneration, MIRA Institute for Biomedical Technology and Technical Medicine, Faculty of Science and Technology, University of Twente, Enschede, the Netherlands

<sup>3</sup> Department of Complex Tissue Regeneration, MERLN Institute for Technology-inspired Regenerative Medicine, Maastricht University, Maastricht, The Netherlands

<sup>4</sup> Center for Neuroscience and Cell Biology, Stem Cells and Drug Screening Lab, University of Coimbra, Coimbra, Portugal

# shared first coauthorship

\* Corresponding author

MERLN Institute for Technology-Inspired Regenerative Medicine,  
Maastricht University

Universiteitssingel 40, Maastricht, 6229 ER,  
The Netherlands

E-mail: [l.moroni@maastrichtuniversity.nl](mailto:l.moroni@maastrichtuniversity.nl)

## Abstract

The fabrication of bioactive scaffolds able to mimic the in vivo cellular microenvironment is a challenge for regenerative medicine. The creation of sites for the selective binding of specific endogenous proteins represents an attractive strategy to fabricate scaffolds able to elicit specific cell response. Here, electrospinning (ESP) and soft-molecular imprinting (soft-MI) techniques were combined to fabricate a soft-molecular imprinted electrospun bioactive scaffold (SMIES) for tissue regeneration. Scaffolds, functionalized using different proteins

and growth factors (GFs), arranged onto the surface, were designed, fabricated and validated with different polyesters, demonstrating versatility of the developed approach. The scaffolds bound selectively each of the different proteins used, indicating that the soft-MI method allowed fabricating high affinity binding sites on ESP fibers compared to non-imprinted ones. The imprinting of ESP fibers with several GFs resulted in a significant effect on cell behavior. FGF-2 imprinted SMIES promoted cell proliferation and metabolic activity. BMP-2 and TGF- $\beta$ 3 imprinted SMIES promoted cellular differentiation. These scaffolds could be used in a cell-free approach to steer endogenous tissue regeneration in several regenerative medicine applications.

**Keywords:** soft-MI, molecular imprinting, electrospinning, mesenchymal stromal cells

## 1 Introduction

In regenerative medicine, scaffolds should act as biocompatible and biodegradable substrates to promote cell attachment, penetration, proliferation and ECM deposition, and should have the proper surface chemistry and topography to sustain tissue development [1].

Synthetic polymers are commonly used for the fabrication of scaffolds due to their high processing flexibility, controllable degradation rates and suitable mechanical properties. However, they lack different biological features needed for tissue regeneration, such as natural cell binding sites. Consequently, cell adhesion on scaffolds made by synthetic polymers occurs via ECM molecules unspecifically adsorbed on their surfaces [1, 2]. In order to guide cell behavior and tissue formation, significant efforts have been made to fabricate functionalized scaffolds to promote cell/material interaction. These interactions require biomolecular recognition of materials by cells, which can be manipulated by the fabrication parameters of the biomaterials, such as modifying the bulk structure or surface with bioactive molecules [1, 3]. In the former, biomolecules are incorporated into the biomaterial and the recognition sites are present on the bulk structure. In the latter, biomolecules are immobilized

on the surface of the biomaterial and the recognition sites are only on the surface [3, 4]. However, bulk modification is not an efficient method to incorporate biomolecules because cell–material interactions take place on scaffold surfaces and the biomolecules encapsulated inside the scaffold are not able to interact with cells [1]. For this reason, surface modification is preferred to fabricate bioactive scaffolds [1].

Currently, several techniques have been developed to modify the surface of scaffolds including physical coating and blending [5], plasma treatment [6,7], graft polymerization, and wet chemical methods [5]. Limitations include: poor controllability (coating), alteration of the bulk properties (blending, and wet chemical methods), limited shelf-life (plasma treatment).

Molecular imprinting (MI) technology represents a novel possibility to obtain molecular recognition sites in polymer structures.

It is a synthetic approach to design robust molecular recognition materials able to mimic natural recognition entities, such as antibodies and biological receptors [12]. Template molecules, crosslinked to a polymer and subsequently removed, impart molecular memory into the biomaterial, which selectively binds to the imprinted template molecules.

MI polymers (MIPs) have been used for specific recognition of different molecules such as drugs and peptides. However, protein imprinting had a limited success due to their large molecular size [13]. Different studies used conventional methacrylate chemistries to prepare protein MIPs [14]. The major limitation of this approach is related to the use of solvents. Furthermore, proteins are insoluble in non-aqueous media and their conformation is strongly modified, influencing in this way the efficiency of the MIPs [15]. Imprintable hydrogels represent a suitable alternative based on protein encapsulation to fabricate delivery agents, but different studies demonstrated that it is possible only for small molecules [16]. 3D sol-gel protein imprinting represents another alternative for the fabrication of MI structures able to recognize specific template molecules. Sol-gel can interact with a variety of proteins for their encapsulation, because a sol-gel reaction is suitable for imprinting proteins due to the mild

polymerization conditions and water compatibility [16]. However, the bulk imprinting of proteins is limited by the sol-gel dense structure and the requirements of grinding to expose binding sites [15]. A novel method of protein imprinting was demonstrated by Umeno et al. who used a polymer coated DNA strand for protein recognition, but the practical use of this method is limited by the high complexity [16].

These methods for protein imprinting demonstrated the potential of MI technologies for different applications such as specific protein entrapment and separation [15]. However, their use in the regenerative medicine field is still partially unknown due to the restrictions related to the biocompatibility requirements and to the structural and mechanical properties of the scaffolds [17].

Rosellini et al. proposed a bioactive scaffold with fibronectin recognition nanosites based on MI [18]. The imprinted particles showed good performance in terms of recognition capacity, quantitative rebinding and selectivity, and were used to functionalize synthetic polymeric films by deposition on their surface. The deposition of the imprinted particles did not alter their specific recognition and rebinding behavior and the functionalized materials promoted cell adhesion and proliferation. Nevertheless, a possible application in regenerative medicine is far to be achieved because the structural and mechanical properties of these structures are strongly different from the tissue ones. Vozzi et al. proposed the Soft-MI technique, which integrates MI and soft lithography, to enhance specific cell response due to the presence of highly specific recognition sites on well-defined microstructures [19]. PMMA scaffolds with a specific microstructure were fabricated via casting and imprinted with different proteins. However, this method did not mimic the fibrous nanoarchitecture of a soft tissue.

In regenerative medicine, the possibility to tailor the scaffold structural and mechanical properties and to functionalize its surface with bioactive agents represents a fundamental option to mimic the hierarchical aligned structure of the native tissues. In this sense, patterned

electrospun fibers represent a suitable technique to replicate the ligament micro- and nano structures [20].

Chronackis et al. developed a simple method to create recognition sites on electrospun fibers [21]. A solution of poly(ethylene terephthalate) (PET) and polyallylamine in the presence of an herbicide as a template molecule, 2,4-dichlorophenoxyacetic acid (2,4-D), was used to fabricate the imprinted electrospun nanofibers. When the template was removed by solvent extraction, imprinted binding sites were left in the nanofiber materials that were capable of selectively rebinding the target molecule. The rebound capacity in the case of imprint nanofibers was 5 times higher than the one showed by non-imprinted nanofibers.

Here, we combine soft-MI and ESP, which we denoted as “SMIES”, to fabricate novel bioactive scaffolds based on polylactic-co-glycolic acid (PLGA), specifically tailored for ligament TE [20]. We then fabricated scaffolds based on poly(ethylene oxide terephthalate)/poly (butylene terephthalate) (PEOT/PBT) and poly-L-D-lactic acid (PLDLA), which also showed the capability to selectively bind a specific template molecule (described in the additional materials).

Together, these studies demonstrate that our novel SMIES technique can be used to fabricate diverse, bioactive scaffolds that mimic an in vivo cellular microenvironment, with diverse potential for broad regenerative medicine applications.

## **2 Experimental Section**

### **2.1 SMIES fabrication**

The fabrication method of SMIES consists of three main steps: fabrication and functionalization of polydimethylsiloxane (PDMS) mold, and fabrication of the scaffold by ESP (**Figure 1**).

#### **2.1.1 Fabrication of the PDMS mold**

The PDMS mold fabrication and functionalization followed the protocol described by Bhatia et al. [22] and Vozzi et al. [19], respectively.

The negative photoresist NANOTM SU-8 50 (MicroChem, Newton, MA) was spin-coated on the silicon wafer, pre-baked to remove the solvent, aligned with a mask aligner (NL-CLR-EV620 Maskaligner) and exposed to UV rays in contact mode. Subsequently, a post-exposure bake to complete the polymerization of the photoresist and a development phase to remove unexposed material were performed. The mask was designed using the software CleWin 4.0 and printed on a transparency using a commercial Linotronic-Hercules 3300-dpi, high-resolution line printer. The mask was divided into seven structures and a pattern composed by lines with a length of 100  $\mu\text{m}$  and a line distance of 50  $\mu\text{m}$  was chosen. The PDMS mold was prepared using a commercial product (Sylgard 184 kit, Dow Corning, MI) with a 10:1 (w/w) ratio. The solution was centrifuged for 1 min at 300 rpm, casted onto the master, degassed, and finally cured in an oven for 4 h at 70 °C. Finally, the master was separated from PDMS and the mold was then washed with 70% ethanol (Sigma Aldrich, The Netherlands), and subsequently with deionized MilliQ water to eliminate impurities.

#### **2.2.2 Functionalization of the PDMS mold**

The functionalization of the PDMS mold was performed using the method described by Vozzi et al. [19]. First, the mold was washed with acetone (Sigma Aldrich, The Netherlands). After evaporation, it was immersed in Piranha Solution ( $\text{H}_2\text{SO}_4/\text{H}_2\text{O}_2$ , 3:1 v/v) for 30 seconds to reduce the hydrophobicity of its surface, and subsequently washed with deionized water.

After the modification of its surface wettability, the PDMS mold was derivatised with a 1% v/v solution of (3-Aminopropyl)-trimethoxysilane (APTS) (purity  $\leq$  97%, Sigma Aldrich, The Netherlands) in Toluene anhydrous 99.8% (Sigma Aldrich, The Netherlands). Toluene was used as a solvent because of its capacity to create a monomolecular layer of silanes on the PDMS surface. The mold was immersed in the APTS solution for 1 h in order to introduce amino groups on its surface to promote protein binding. Subsequently, the mold was washed three times with toluene to remove any excess of silane, and dried in an oven at 40 °C for 1 h to ensure the complete evaporation of the solvent.

The activation of the functional groups of the silanized surface was promoted by dipping the mold for 1 h into an aqueous solution (pH = 6.4) of 2 mM hydroxysuccinimide (NHS) (purity  $\geq$  98.0%, Sigma Aldrich, The Netherlands), and 5 mM dimethylaminopropyl-ethyl-carbodiimide (EDC) (purity = 97%, Aldrich, The Netherlands). This step allowed the reaction between the nucleophilic groups present on the PDMS mold and the carboxylic groups of the protein and vice versa, the carboxylic groups present on the PDMS mold and nucleophilic groups of the protein [23]. Then, the mold was washed with deionized water to remove any excess reagent.

The PDMS mold was immersed in a solution of the template protein at 4 °C in the dark. After 24 h, the mold was washed with deionized water to remove any excess protein.

FITC-albumin and TRITC-lectin (Sigma- Aldrich, The Netherlands) were initially used as template model molecules for the MI of electrospun scaffolds, for evaluating the binding activity, from Sigma-Aldrich. Deionized water solutions of FITC-albumin and TRITC-lectin at concentrations of 1  $\mu$ g/ml in deionized water were prepared.

After the demonstration of the proof-of-concept with fluorescent molecules, the PDMS mold was functionalized with the Growth Factors (GFs) FGF-2 (Neuromics), TGF- $\beta$ 3 or BMP-2 (R&D Systems), for application in ligament tissue engineering. Deionized water solutions (one for each GFs) at a concentration of 10 ng/ml were prepared.

### **2.2.3 Electrospinning process**

The functionalized PDMS mold was used as a target for the ESP jet. SMIES were fabricated using a 4% w/v PLGA (Boehringer-Ingelheim) solution in 1,1,1,3,3,3-hexafluoro-2-propanol (HFIP) (Sigma Aldrich, The Netherlands).

ESP was performed in an environmental chamber with a controlled temperature of 25 °C and a relative humidity of 30%. The polymer solution was loaded into a 5ml syringe (BD Biosciences) and pumped using a syringe pump (KDS-100-CE, KD Scientific) through a Teflon tube connected to a stainless steel needle (0.5 mm inner diameter, 0.8 mm outer diameter). The needle was mounted in a 30 x 20 cm upper parallel plate and centered on a custom made collector composed by two flat aligned electrodes.

The functionalized PDMS mold was positioned under the ESP jet, on the top of the two aligned electrodes, and the ESP fibers fabricated at a flow rate of 1ml/h, a voltage of 20 kV and a needle-collector distance of 20 cm. These parameters were chosen after an optimization process (data are not shown). The ESP fiber density was determined as the time frame used during fabrication, which was set to 4 hours.

## **2.2 Scaffold characterization**

Details on morphological and mechanical characterization are given in supporting information, as not specifically developed for SMIES. Investigations include scanning electron microscopy, porosity, permeability, surface wettability, surface roughness, uniaxial tensile and stress relaxation tests and their explanation using the modified Quasi Linear Viscoelasticity model (mQLV) [24].

## **2.3 Rebinding ability and selective recognition analysis**

In order to evaluate the rebinding ability and the selectivity for the template molecule (FITC–albumin or TRICT–lectin), the imprinted scaffolds (n = 3) were dipped in three different aqueous solutions: FITC–albumin (1 µg/ml), TRITC–lectin (1 µg/ml) and both proteins (1:1, 1 µg/ml). The obtained SMIES were washed 3 times with water and analyzed by fluorescence



microscope (non-inverted NIKON E600) to ensure that no weakly bound protein on the PDMS was transferred to them. A Texas Red filter (excitation wavelength 542–576 nm, emission wavelength 600–675 nm) and a FITC filter (excitation wavelength 488–495 nm, emission wavelength 519 nm) were used to distinguish lectin and albumin, respectively. Pictures were taken with a Nikon DS-Fi1c camera equipped with NIS-Element software.

#### **2.4 GF imprinting quantification**

The quantification of the rebound BMP-2 and TGF- $\beta$ 3 growth factors was performed through an enzyme-linked immunosorbent assay (ELISA, R&D systems). Briefly, after the imprinting procedure, the supernatant containing the soluble GF was collected to quantify the amount of unlinked protein. The GF left in the supernatant from a control scaffold (not imprinted) was also quantified to determine nonspecific protein adsorption. The imprinting efficiency ratio was defined as the ratio between the signal of the target molecule obtained with the imprinted scaffold and the signal of the target molecule obtained with a non-imprinted scaffold, under the same conditions [25].

BMP-2 and TGF- $\beta$ 3 were quantified using an ELISA assay according to the manufacturer's instructions (DY355-05 and DY243, respectively).

#### **2.5 Cell expansion and culture conditions**

Different biological investigations were performed to validate the imprinted PLGA SMIES. The scaffolds for cell culture experiments were produced as before, punched into 22 mm discs to fit inside a sterile, non-treated 12-well plate (NUNC). Viton® polymer rings (Eriks b.v., The Netherlands), with an outer diameter of 22 mm and an inner diameter of 19.6 mm, were sterilized in 70% ethanol and inserted into the wells to hold the scaffolds to the bottom. The rings also served to confine seeded cells to the scaffold only. Subsequently, the scaffolds were sterilized in 70% ethanol for 15 minutes, washed twice in PBS solution (Gibco-BRL) for 5 minutes, and incubated in proliferation medium overnight to pre-wet the scaffold and promote protein adsorption. Three different cell types were used, according to the imprinted growth

factor: human mesenchymal stromal cells (hMSCs) for FGF-2, mink lung epithelial cells (MLECs) for TGF- $\beta$ , and mouse myoblast cells for BMP-2. Details of culture conditions of each cell type is given in the supplementary information.

## **2.6 Cell Imaging - Scanning electron microscopy**

Cell attachment and distribution were observed after 7 days of culture using a Philips XL ESEM-FEG. Briefly, SMIES were rinsed twice with PBS and fixed in 10% formalin for 15 minutes. Subsequently, the samples were dehydrated in sequential ethanol series (50%, 60%, 70%, 80%, 90%, 96% and 100%), 15 minutes for each concentration. For the final dehydration step, scaffolds were immersed in hexamethyldisilazane (Sigma-Aldrich, The Netherlands) and the solvent was left to evaporate overnight. Finally, samples were gold sputter-coated (Cressington Sputter Coater 108 auto) prior to analysis by the SEM. Images were obtained under high vacuum with an acceleration voltage of 10 kV and a working distance of 10 mm.

## **2.7 Cell Imaging - Fluorescence microscopy**

Fluorescence analysis was performed to evaluate cell morphology and distribution after 1, 3 and 7 days of culture. Scaffolds were rinsed twice with PBS and fixed in 10% formalin for 15 minutes. Cell membranes were permeabilised with 0.25% (v/v) Triton X-100 (Sigma-Aldrich) in PBS for 5 min, followed by rinsing in PBS, 3 times for 5 minutes. Non-specific binding was blocked using 1% (w/v) BSA in PBS. Nuclei were labeled by incubating the samples with 100 ng/mL of 4',6' Diamidin-2'-phenylindoldihydrochlorid (DAPI, Sigma, Munich, Germany) in PBS for 20 minutes. After rinsing the sample 3 times with PBS, actin filaments were stained with 200 ng/ml of Phalloidin (Alexa Fluor 594 Phalloidin, Invitrogen) for 1 hour to visualize the cytoskeleton. Samples were rinsed 3 times, stored in the dark, and subsequently analyzed on a fluorescence microscope (Nikon Eclipse E600). A BFP filter (excitation wavelength 379–401 nm, emission wavelength 438–485) was used for DAPI staining and a Texas Red filter (excitation wavelength 542–576 nm, emission wavelength

600–675 nm) for phalloidin. Pictures were taken with a Nikon DS-Fi1c camera equipped with NIS-Element software.

## **2.8 Biochemical investigations**

### **Presto blue assay**

Presto blue assay (Life technology, The Netherlands) was performed to evaluate the influence of FGF-2 imprinted scaffolds on metabolic activity after 1, 3 and 7 days of culture. Briefly, the cell permeable resazurin-based solution provided was diluted 10 times in the same type of medium in which cells were cultured, according to the to the manufacturer's instructions: 1.5 ml of basic medium supplemented with Presto blue reagent was added to each well and incubated for 2 h in the dark at 37 °C in a humidified atmosphere with 5% CO<sub>2</sub>. The reducing power of living cells modified the reagent, which turned red in color. From each sample, 100 µl of medium was transferred in a clear-bottom, 96-well, black plate, and the color change was detected using a spectrophotometer LS50B (Victor 3, Perkin Elmer) according to the manufacturer's instructions. The experiments were performed in triplicate.

### **DNA assay**

In order to quantify the cell number, the amount of DNA was calculated with CyQuant DNA assay kit (Molecular Probes, Invitrogen), according to the manufacturer's instructions, after 7 days of culture. Briefly, the FGF-2-imprinted scaffolds were cut in order to improve the lysis efficiency. Samples were stored at -30 °C and freeze-thawed 5 times. Afterwards, the constructs were digested for 16 hours at 56 °C with 1 mg/ml proteinase K (Sigma Aldrich) in Tris/EDTA buffer (pH 7.6) composed of 18.5 µg/ml of iodoacetamine (Sigma Aldrich) and 1 µg/ml Pepstatin A (Sigma Aldrich). To avoid the interference caused by the binding of the dye to the RNA, 100 µl of the sample were incubated for 1 hour at room temperature with 100 µl of lysis buffer provided by the kit (Component B diluted in 180 mM NaCl, 1 mM EDTA in distilled water in the ratio 1:20), in which RNase enzyme was diluted 1000 times. Quantification of the total DNA was performed using a green fluorescent dye provided by the

kit (excitation 480 nm, emission 520 nm). Fluorescence was measured at 480 nm using a spectrophotometer LS50B (Victor 3, Perkin Elmer), and DNA concentrations were calculated from a  $\lambda$  DNA standard curve.

### **Luciferase assay**

To evaluate the activation of TGF- $\beta$ 3 and BMP-2 signaling pathway induced by the imprinted scaffolds, the reporter cell lines described above were used [26]. In particular, MLECs were used to evaluate TGF- $\beta$ 3 and C2C12 cells were used to monitor the BMP-2 pathway. The scaffolds were imprinted with 10 ng/ml of the respective GF and as controls, nonimprinted scaffolds and imprinted scaffolds in which the media was supplemented with 10  $\mu$ M/well of a GF inhibitor were used. Noggin (Sigma Aldrich, The Netherlands) was used as BMP-2 inhibitor and SB 431542 hydrate (Sigma Aldrich, The Netherlands) as TGF- $\beta$ 3 inhibitor. After seeding, cells were cultured in DMEM (Gibco) supplemented with FBS (10% (w/v), Lonza), penicillin (100 U/ml, Gibco), and streptomycin (100  $\mu$ g/ml, Gibco). After 24 hours, the medium was exchanged with an equal one in which the FBS was not added.

After day 3 of culture, the luciferase assay was performed according to the manufacturer's instructions (PROMEGA Corporation, USA). Briefly, samples were gently washed three times with PBS. Reporter lysis buffer was diluted (1:5), and 1 ml was added to both samples and controls. Subsequently, the plate was covered with aluminium foil and stored at -80 °C. To perform the analysis, 100  $\mu$ l of lysate and luciferase assay buffer were transferred to a white, 96-well plate and analysed using spectrophotometer LS50B (Victor 3, Perkin Elmer) according to the manufacturer's instructions. Luciferase activity, reported as relative light units (RLU), was normalized for the DNA content.

### **2.9 Statistical analysis**

All data are expressed as mean  $\pm$  standard deviation (SD). Biochemical assays were performed on triplicate biological samples. A one-way statistical analysis of variance (ANOVA) with a significance level of  $p < 0.05$  was used to determine differences between

three groups present in the luciferase assay. Tukey's multiple comparisons test was used to perform post hoc analysis. A t-test was performed with a significance level of  $p < 0.05$  to compare results obtained in the other experiments. Statistical significance between the control group and the experimental groups is indicated, with the following designations: \*p-value  $< 0.05$ , \*\*p-value  $< 0.01$ , and \*\*\*p-value  $< 0.001$ .

### 3 Results and discussion

We fabricated PLGA-based SMIES imprinted with FITC–albumin, TRITC–lectin, FGF-2, TGF- $\beta$ 3 or BMP-2. The scaffolds had an interconnected pore network, composed of uniform nanofibers with mean diameters of  $571 \pm 70$  nm, corresponding to a porosity of  $94.2 \pm 2.4\%$ . Their microstructure accurately conforms to the striped pattern of the PDMS mold. The theoretical line width was set to  $100 \mu\text{m}$  (equal to the spacing on PDMS mold) and the experimental one was measured as  $104 \pm 4 \mu\text{m}$ . The theoretical distance between two lines was set to  $50 \mu\text{m}$  and the experimental value was measured as  $65 \pm 9 \mu\text{m}$ .

The SMIES fabrication method did not change the morphological properties of the PLGA scaffolds compared to non-imprinted ESP fabrication. The surface roughness ( $R_q$ ), a measurement for cell and protein attachment, was  $160.2 \pm 32.4$  nm for the imprinted PLGA scaffolds and  $170.4 \pm 50.8$  nm for the non-imprinted ones (**Figure 1D**). The contact angle, measured to assess the wettability of the scaffold surface, was  $130.6 \pm 10.1^\circ$  for the imprinted PLGA scaffolds and  $127.3 \pm 11.1^\circ$  for the non-imprinted ones (**Figure 1E**), with no statistical differences between the two groups. The scaffolds presented a similar permeability [ $\text{L m}^{-2} \text{h}^{-1} \text{bar}^{-1}$ ]:  $38.9 \pm 1.73$  for the imprinted and  $38.6 \pm 1.81$  for the non-imprinted, and a Sieving Coefficient (SC) of  $>0.96$  for BSA (66 kDa) indicating that large proteins permeated freely through the scaffolds.

The similarity of the bulk properties of imprinted and non-imprinted scaffolds was further confirmed by mechanical tests (see supplementary information): no statistically different elastic and viscoelastic properties, including Young Modulus ( $87.50 \pm 21.10$  MPa vs  $90.20 \pm 23.30$  MPa) and relaxations times, were observed. Comparable mechanical properties between the native tissue and the synthetic substitute can promote adequate mechanical stimuli that, together with other factors, can influence cell growth and differentiation. In this case, the imprinted PLGA scaffold showed mechanical and viscoelastic properties that matched the ones of native soft tissues [27]. In particular, the modified quasi-linear viscoelastic (mQLV)

parameters obtained for the PLGA scaffold result in a similar range with the ones of the native ligament soft tissue [24].

With respect to the not-imprinted counterpart, the SMIES demonstrated affinity and selectivity for their template molecule over the other fluorescent protein competitor (**Figure 2**). The FITC-albumin-imprinted PLGA SMIES showed high protein absorption in a solution of FITC-albumin (**Figure 2A**), but minimal adsorption in a solution of TRITC-lectin (**Figure 2B**). When both albumin and lectin were present (1:1) in solution, the albumin-imprinted SMIES bound only albumin (**Figure 2C** and **Figure 2D**). Analogous results were obtained with the TRITC-lectin-imprinted SMIES. Non-imprinted PLGA scaffolds bound neither lectin nor albumin (**Figure 2I-N**).

The quantity of imprinted Growth Factors (GFs) on the SMIES can be evaluated through an indirect measurement with ELISA tests. Results showed that BMP-2-imprinted scaffolds were able to bind significantly more BMP-2 compared to unspecific binding observed on non-imprinted scaffolds (12.4%, efficiency ratio = 1.18, p-value < 0.01; **Figure 2O**; the efficiency ratio is defined in materials and methods). Similarly, TGF- $\beta$ 3-imprinted scaffolds bound 33% more TGF- $\beta$ 3 (efficiency ratio = 1.62) compared to non-imprinted controls (p-value < 0.001, **Figure 2P**).

To evaluate the SMIES' ability to sustain cell proliferation, hMSCs were cultured on the scaffolds and cell morphology and distribution were evaluated after 1, 3 and 7 days (**Figure 3A-B-C**). hMSCs were homogeneously distributed at day 1 on the scaffold surface and started to align along the microstructure at day 3. Cells were well spread and aligned along the microtopographies at day 7. SEM analysis after 7 days of culture also revealed a homogenous distribution of hMSCs on the entire scaffolds and their alignment along the microtopographies (**Figure 3D-G**).

FGF-2 imprinted scaffolds were tested for their ability to promote cell proliferation analyzing cell seeding efficiency (CSE), metabolic activity and cell number after 7 days. The initial cell seeding procedure is a critical step in a TE process. Cell seeding efficiency analysis was performed to exclude the possibility that subsequent changes in proliferation between the FGF-2 imprinted scaffolds and the controls could be due to differences in the initial seeding. CSE was evaluated after 24 hours: for SMIES it was  $29.3 \pm 7.9\%$  and no statistical difference between the SMIES and the controls was found (**Figure 3H**).

The metabolic activity after 1, 3 and 7 days was assessed with Presto blue assay. The FGF-2 imprinted scaffold showed a statistically significant increase of the metabolic activity for each time point compared to the control (**Figure 3I**). The DNA quantification after 7 days of cell culture confirmed the trend presented in the metabolic activity analysis, showing a statistically significant increase of proliferation on FGF-2 imprinted scaffolds compared to the control (**Figure 3L**). These results suggest that FGF-2 present onto the SMIES s was capable of eliciting the expected pro-mitogenic effect on hMSCs ultimately leading to a higher number of cells compared to the control.

In order to evaluate the effective presence and bioactivity of the imprinted BMP-2 and TGF- $\beta$ 3, a luciferase assay was performed with specific reporter cell lines. In this test, an increase in luciferase activity corresponds to an increase on BMP-2 and TGF- $\beta$ 3 signaling. Luciferase activity was normalized for the DNA content to correct for the total cell number in the scaffolds. As showed in **Figure 3M-N**, SMIES presented a higher luciferase activity compared to the controls and to the SMIEs with the addition of specific inhibitors of BMP-2 and TGF-  $\beta$ 3, suggesting that the imprinted scaffolds were able to bind and present the respective GFs to the reporter cell line.

The imprinting of ESP fibers with several GFs resulted in a significant effect on cell behavior. In particular, FGF-2 promoted cell proliferation and FGF-2 SMIES showed a statistically



higher metabolic activity over the time and a higher number of cells after 7 days. BMP-2 and TGF- $\beta$ 3 SMIEs showed a statistically higher luciferase signal that demonstrated the presence and the bioactivity of GFs binding domains.

## **4 Conclusion**

The presented research shows for the first time the possibility to imprint nanofibers to create bioactive ESP scaffolds for regenerative medicine applications. Future investigations will focus on the optimization of the imprinting procedure to improve the efficiency of the process, on imprinted GF release analysis over time, and on further characterization on GFs' influence on cell differentiation. Moreover, the possibility to imprint a "mimic analog peptide" able to replicate the "imprinting site" of specific GFs represents a fascinating improvement in order to reduce the manufacturing costs and fabricate a completely synthetic imprinted scaffold able to selectively bind a targeted protein. In addition, an innovative approach could be represented by "direct cell imprinting", in which cells can be used as template structure to imprint ESP fibers.

In conclusion, the integration of ESP and soft-MI represents a powerful and promising technique for the fabrication of scaffolds for regenerative medicine applications, because it allows us to get one step closer to mimic the structural environment of tissues.

## **Acknowledgements**

This research project has been made possible with the support of the Dutch Province of Limburg. Some of the materials used in this work were provided by the Texas A&M Health Science Center College of Medicine Institute for Regenerative Medicine at Scott & White through a grant from NCRP of the NIH (Grant #P40RR017447).

## 5 References

- [1] X. Liu, J.M. Holzwarth, P.X. Ma, Functionalized synthetic biodegradable polymer scaffolds for tissue engineering. *Macromol. Biosci.* **2012**, 12, 911–9.
- [2] J. Venugopal, Y.Z. Zhang, S. Ramakrishna, Fabrication of modified and functionalized polycaprolactone nanofibre scaffolds for vascular tissue engineering. *Nanotechnology* **2005** 16, 2138–42.
- [3] H. Shin, S. Jo, A.G. Mikos, Biomimetic materials for tissue engineering. *Biomaterials* **2003**, 24, 4353–64.
- [4] J. Crispim, H.A.M. Fernandes, S.C. Fu, Y.W. Lee, P. Jonkheijm, D.B.F. Saris, TGF- $\beta$ 1 activation in human hamstring cells through growth factor binding peptides on polycaprolactone surfaces. *Acta Biomater.* **2017**, 53 165–78
- [5] H. Chen, R.K. Truckenmuller, C.A. van Blitterswijk, L. Moroni. Fabrication of nanofibrous scaffolds for tissue engineering applications. In: *Nanomaterials in tissue engineering: Fabrication and applications. Series in Biomaterials (56)*. Woodhead Publishing, 2013 158 - 182. ISBN 9780857095961
- [6] X. Zhu, K.S. Chian, M.B.E. Chan-Park, S.T. Lee, Effect of argon-plasma treatment on proliferation of human-skin-derived fibroblast on chitosan membrane in vitro. *J. Biomed. Mater. Res. A* 2005 73, 264–74.
- [7] R. Morent, N. De Geyter, T. Desmet, P. Dubruel, C. Leys. Plasma Surface Modification of Biodegradable Polymers: A Review. *Plasma Process. Polym.* 2011, 8, 171–190.
- [8] G. Vasapollo, R. Sole, L. Del Mergola, M.R. Lazzoi, A. Scardino, S. Scorrano, G. Mele, Molecularly imprinted polymers: present and future prospective. *Int. J. Mol. Sci.* 2011, 12, 5908–45.
- [13] X. Zhou, W. Li, X. He, L. Chen, Y. Zhang, Recent Advances in the Study of Protein Imprinting *Sep. Purif. Rev.* **2007**, 36, 257.
- [14] G. Wulff, Molecular Imprinting in Cross-Linked Materials with the Aid of Molecular Templates— A Way towards Artificial Antibodies. *Angew. Chemie Int. Ed. English* **1995**, 34, 1812.
- [15] N. W. Turner, C. W. Jeans, K. R. Brain, C. J. Allender, V. Hlady, D. W. Britt, From 3D to 2D: a review of the molecular imprinting of proteins. *Biotechnol. Prog.* **2006**, 22, 1474.
- [16] I. Gill, A. Ballesteros, Bioencapsulation within synthetic polymers (Part 1): sol-gel encapsulated biologicals. *Trends Biotechnol.* **2000**, 18, 282.

- [16] D. Umeno, M. Kawasaki, M. Maeda, Imprinting of proteins on polymer-coated DNA for affinity separation with enhanced selectivity. In: Bartsch, RA.; Maeda, M., editors. *Molecular and Ionic Recognition with Imprinted Polymers*. Washington DC: American Chemical Society; **1998**. p. 202-216. ACS Symposium Series 703 51.
- [17] M. I. Neves, M. E. Wechsler, M. E. Gomes, R. L. Reis, P. L. Granja, N. A. Peppas, Molecularly Imprinted Intelligent Scaffolds for Tissue Engineering Applications. *Tissue Eng. Part B Rev.* **2017**, *23*, 27.
- [18] E. Rosellini, N. Barbani, P. Giusti, G. Ciardelli, C. Cristallini, Novel bioactive scaffolds with fibronectin recognition nanosites based on molecular imprinting technology. *J. Appl. Polym. Sci.* **2010**, *118*, 3236.
- [19] G. Vozzi, I. Morelli, F. Vozzi, C. Andreoni, E. Salsedo, A. Morachioli, P. Giusti, G. Ciardelli, SOFT-MI: a novel microfabrication technique integrating soft-lithography and molecular imprinting for tissue engineering applications. *Biotechnol. Bioeng.* **2010**, *106*, 804.
- [20] G. Criscenti, A. Longoni, A. Di Luca, C. De Maria, C. A. van Blitterswijk, G. Vozzi, L. Moroni, Triphasic scaffolds for the regeneration of the bone-ligament interface. *Biofabrication* **2016**, *8*, 15009.
- [21] I. S. Chronakis, B. Milosevic, A. Frenot, L. Ye, Generation of Molecular Recognition Sites in Electrospun Polymer Nanofibers via Molecular Imprinting. *Macromolecules* **2006**, *39*, 357.
- [22] S. N. Bhatia, C. S. Chen, Tissue engineering at the micro-scale. *Biomed. Microdevices* **1999**, *2*, 131.
- [23] F. Bianchi, G. Vozzi, C. Pescia, C. Domenici, A. Ahluwalia, A comparative study of chemical derivatisation methods for spatially differentiated cell adhesion on 2-dimensional microfabricated polymeric matrices. *J. Biomater. Sci. Polym. Ed.* **2003**, *14*, 1077.
- [24] S. D. Abramowitch, S.L. Woo, An Improved Method to Analyze the Stress Relaxation of Ligaments Following a Finite Ramp Time Based on the Quasi-Linear Viscoelastic Theory. *J. Biomech. Eng.* **2004**, *126*, 92.
- [25] S.-W. Lee, T. Kunitake, *Handbook of Molecular Imprinting: Advanced Sensor Applications*, Pan Stanford Publishing (September 18, 2012), **2012**.
- [26] M. Abe, J. G. Harpel, C. N. Metz, I. Nunes, D. J. Loskutoff, D. B. Rifkin, An assay for transforming growth factor-beta using cells transfected with a plasminogen activator inhibitor-1 promoter-luciferase construct. *Anal. Biochem.* **1994**, *216*, 276.

[27] G. Criscenti, C. De Maria, E. Sebastiani, M. Tei, G. Placella, A. Speziali, G. Vozzi, G. Cerulli, Quasi-linear viscoelastic properties of the human medial patello-femoral ligament. *J. Biomech.* **2015**, *48*, 4297

## Figures and figure legends

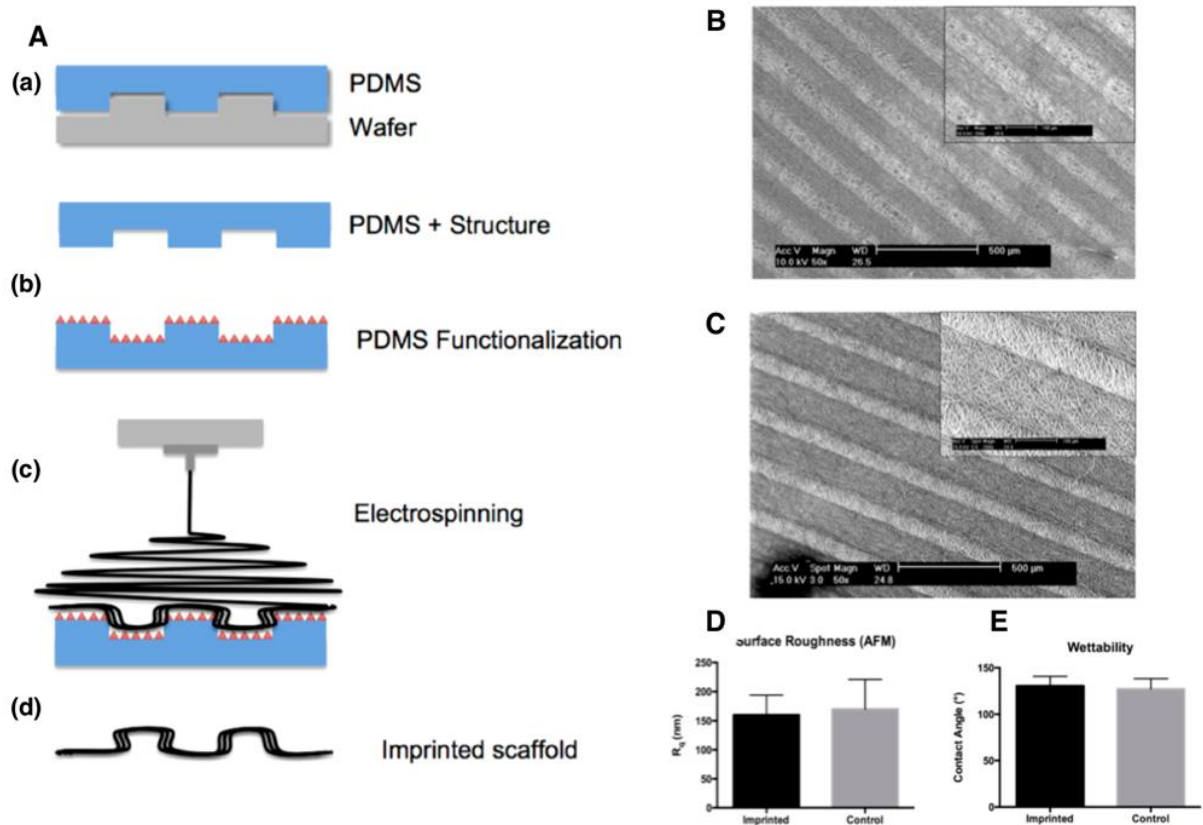


**Figure 1.** SMIES fabrication process (A): (a) Soft-lithography process for the fabrication of PDMS mold; (b) functionalization of PDMS mold by chemical treatment (piranha solution, derivatization with APTES, activation with EDC-NHS solution and incubation with a template protein); (c) ESP of the polymer solution on top of the functionalized PDMS mold; (d) removal of the electrospun scaffold from the mold to obtain the imprinted scaffold (i.e. SMIES). Morphologic characterization of SMIES: microtopography shows uniform nanofibers and striped microstructure (inset, scale bar: 100  $\mu$ m) (B) and the control (not imprinted scaffold) that shows similar uniform nanofibers and striped microstructure (inset, scale bar: 100  $\mu$ m) (C); surface roughness ( $R_q$ , at scan size of 1  $\mu$ m) (D) and wettability (determined by contact angle) were similar for SMIES and non-imprinted PLGA scaffolds (control) (E).

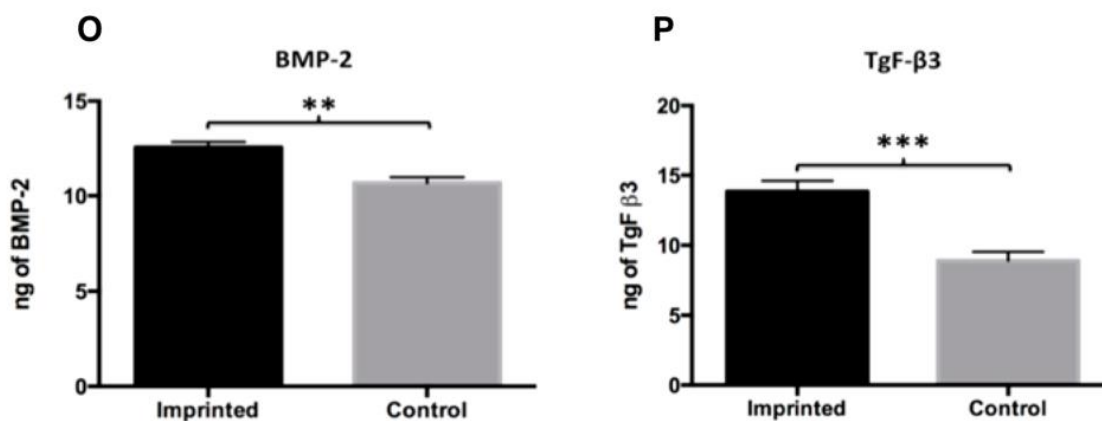
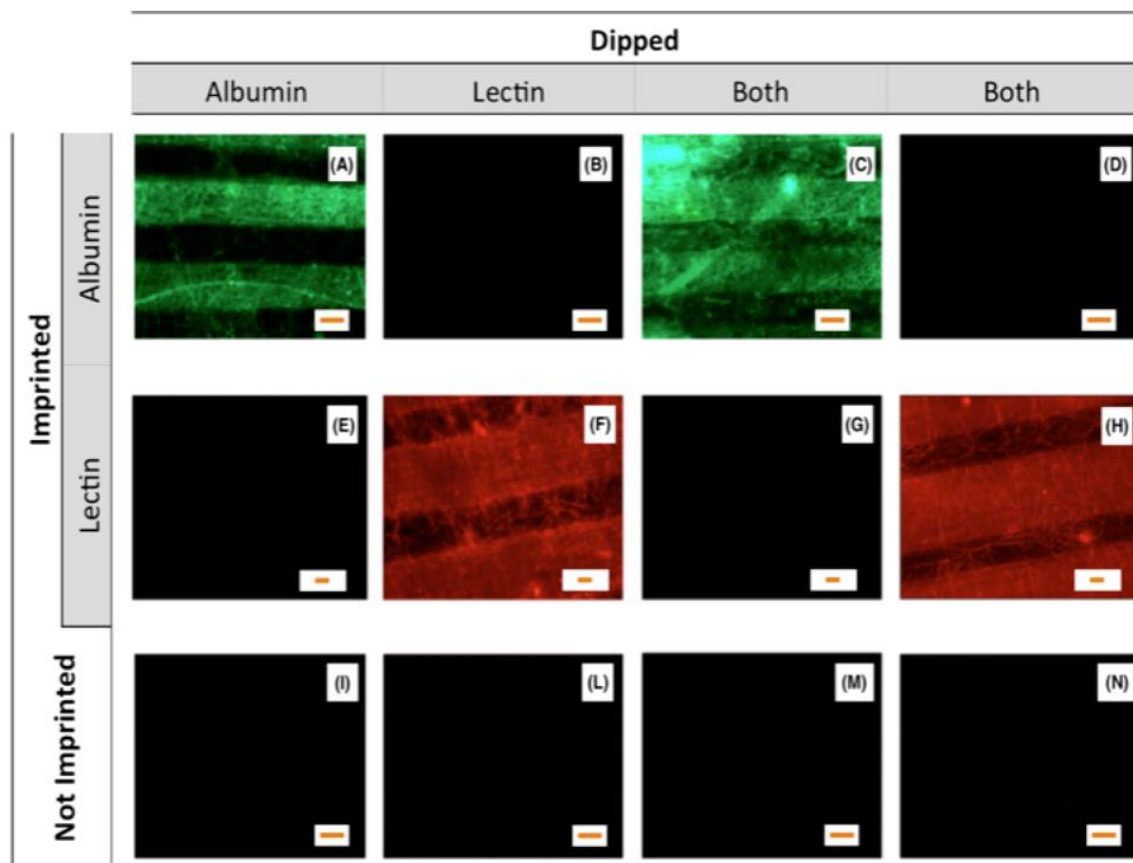


**Figure 2.** SMIES (A) imprinted with FITC-albumin dipped in FITC-albumin; (B) imprinted with FITC-albumin dipped in TRITC-lectin; (C-D) imprinted with FITC-albumin dipped in both proteins; (E) imprinted with TRITC-lectin dipped in FITC-albumin; (F) imprinted with TRITC-lectin dipped in TRITC-lectin; (G-H) imprinted with TRITC-lectin dipped in both protein; (I) un-imprinted PLGA scaffold dipped in FITC-albumin; (L) control (non-imprinted PLGA scaffold) dipped in TRITC-lectin; (M-N) control dipped in both proteins. Fluorescence microscopy of SMIES and control shows selective binding to the respective templated molecules. SMIES were imprinted with either FITC-albumin (top row) or TRICT-lectin (middle row), then dipped into solutions containing albumin (first column), lectin (second column) or both proteins (1:1, two right columns) before analysis. Controls showed no binding to either protein (bottom row). Scale bar: 100 um. Quantification of imprinted GFs on SMIES compared to controls (O-P \*\* p-value < 0.01, \*\*\* p-value < 0.001).

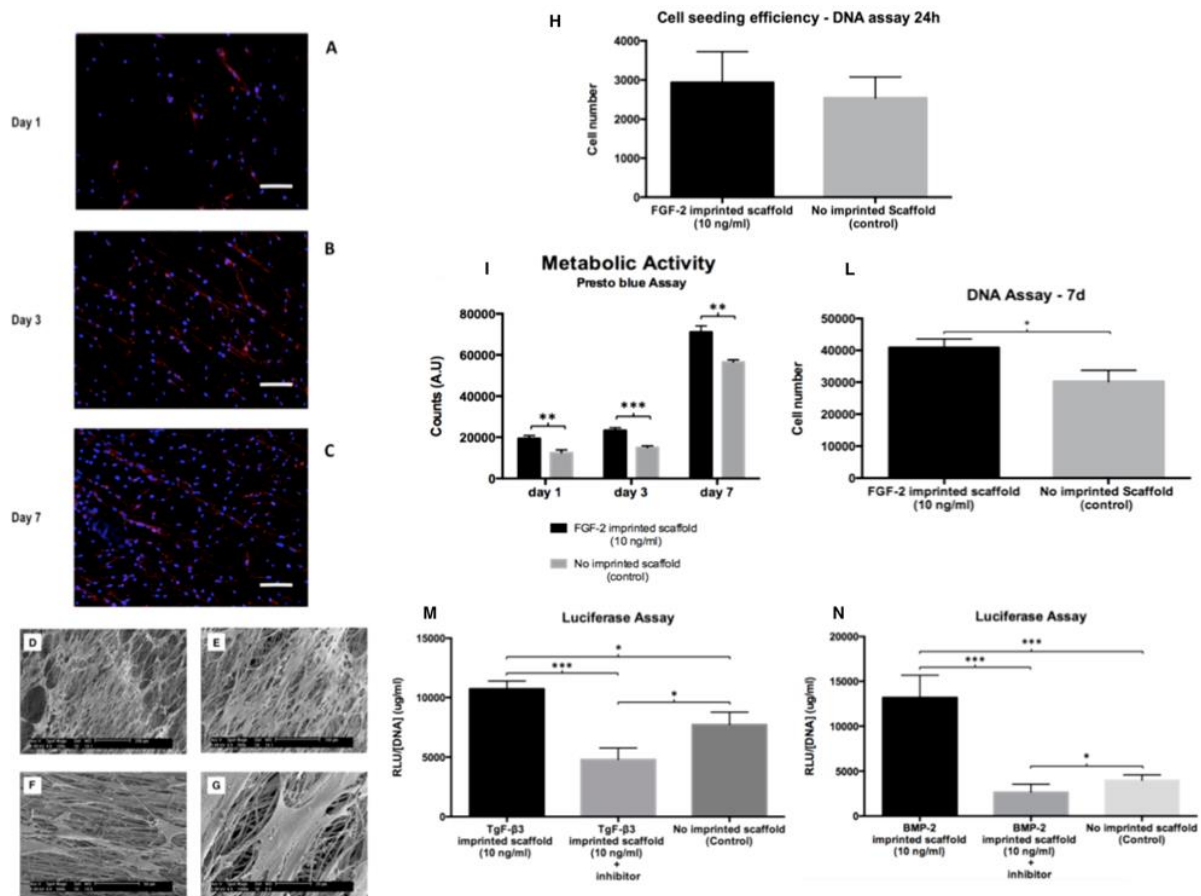


**Figure 3.** hMSCs proliferate and align on FGF-2-SMIES, as visualized by fluorescence microscopy (A-C) and SEM (D-G) after day 1 (A), day 3 (B), and day 7 (C-G) of culture. Scale bars represent 200  $\mu\text{m}$  (D), 100  $\mu\text{m}$  (A-C, E), 50  $\mu\text{m}$  (F), and 20  $\mu\text{m}$  (G); Cell seeding efficiency of FGF-2 SMIES (H) Metabolic activity of FGF-2 SMIES after 1, 3 and 7 days (I) and proliferation analysis of FGF-2 SMIES after 7 days of culture (L); Luciferase activity measured using a TGF reporter cell line for TGF- $\beta$ 3 SMIES (M) and BMP reporter cell line for BMP-2 (N) SMIES